



Assessment of two methods on zoning wildfire propagation in Itacolomi State Park, Minas Gerais State, Brazil

Vicente Paulo Santana Neto^{1*}, David Marques Soares², Thaís Camargos da Silva¹, Fillipe Tamiozzo Pereira Torres¹

¹Universidade Federal de Viçosa, Departamento de Engenharia Florestal, Avenida Purdue, Campus Universitário, CEP 36570-900, Viçosa, MG, Brasil

²Universidade Federal de Ouro Preto, Departamento de Engenharia Ambiental, Campus Universitário, CEP 35440-000, Ouro Preto, MG, Brasil

*Corresponding author:
vipsneto@gmail.com

Index terms:

Forest fires
Methodology
Geographical information systems

Termos para indexação:

Incêndio florestal
Metodologia
Sistema de informação geográfica

Abstract - This study aimed to assess the wild fire propagation risk to wildfires in the Itacolomi State Park, in Minas Gerais State, Brazil, using GIS and to compare the efficiency of the incident solar radiation over the aspect variable. The following variables were used: land cover/use (LCU), slope (SLP), slope curvature (CUR), aspect (ASP) and incident solar radiation (SOL). The weights of each variable were calculated from the ratio between the total area and the burned area of each class in order to generate the fire propagation risk maps. Fire data from 2016 to 2019 were used for validation. When the moderate risk class was considered susceptible, inadequate precision was observed for both methods (ASP and SOL). On the other hand, when the moderate class was considered non-susceptible to fire, the results presented moderate accuracy. Furthermore, the methods using SOL and ASP showed similar results. The results can guide fire mitigation actions on the park.

Received in 08/11/2021
Accepted in 11/03/2022
Published in 21/06/2023

Avaliação de dois métodos para o zoneamento de propagação de incêndios florestais no parque estadual de Itacolomi, Estado de Minas Gerais, Brasil

Resumo - Este estudo teve por objetivo avaliar o risco de propagação de incêndios florestais no Parque Estadual do Itacolomi, MG, utilizando ambiente SIG, e comparar a eficiência da radiação solar incidente com a variável aspecto. Foram utilizadas as seguintes variáveis: uso / cobertura do solo (LCU), declividade (SLP), curvatura do declive (CUR), aspecto (ASP) e radiação solar incidente (SOL). Os pesos de cada variável foram calculados a partir da razão entre a área total e a área queimada de cada classe, para gerar os mapas de risco de propagação de fogo. Dados de incêndios de 2016 a 2019 foram usados para validação. Quando a classe de risco moderado foi considerada suscetível, a precisão inadequada foi observada para ambos os métodos (ASP e SOL). Por outro lado, quando a classe moderada foi considerada não suscetível ao fogo, os resultados apresentaram acurácia moderada. Além disso, os métodos utilizando o SOL e o ASP apresentaram resultados semelhantes. Os resultados podem nortear as ações de mitigação de incêndios no parque.



Introduction

Wildfires are a global problem, and it has increasingly affected areas due to high rates of urbanization and other changes in land use and occupation, such as the expansion of agriculture and livestock (Sarricolea et al., 2020). Wildfires can be defined as unwanted fires that occur in any type of vegetation, including abandoned agricultural land and rural areas with vegetation (Leuenberger et al., 2018).

The number of fires has significantly increased, mainly in tropical ecosystems, causing environmental, economic and social negative impacts (Kayet et al., 2020). Among the affected areas, protected areas are of great concern, which has led to the search for better methods to prevent fire (ICMBio, 2021).

Eugenio et al. (2016) highlighted that forest fire risk maps consist on a basic element for planning and protection of forest. The ability to recognize which places are most likely to have a forest fire outbreak in a given area, under particular environmental and human conditions, is a modern tool to support forest protection plans and reduce the consequences of fires, which can also affect neighboring areas. It also allows the adoption of strategies aimed at preventing such events (Leuenberger et al., 2018; Marchesan et al., 2020).

According to Guglietta et al. (2015), fire risk maps can guide the allocation of fire detection systems and resources for fighting fires, in addition to assist in the categorization and regulation of risky activities on the most prone areas. Furthermore, it can support integrated fire management strategies, such as the prescribed burning at the beginning of the dry season, which reduces both the burned area and the severity, and consequently the amount of greenhouse gas emissions (Edwards et al., 2018).

Therefore, many research works aim to assess wildfire propagation risk, using different methods for the development of forest fire risk zoning maps, linking the environmental factors of a region with its potential to wildfire and enabling the mapping of the fire risk potential according to the sensitivity of the analyzed factors related to fire (Eugenio et al., 2016).

In this context, the geographic information system (GIS) assists the detection of the more fire prone areas, since it informs the spatial distribution of wildfires and improves prevention strategies (Leal et al., 2019). Another characteristic is the possibility of integrate and evaluate diverse information from the study area, such

as type of vegetation, soil and slope. Therefore, since the occurrence of fires is the result of complex non-linear interactions between natural and anthropogenic forces (Guglietta et al., 2015), it is necessary to use methods able to efficiently assess the contribution of the different criteria analyzed to the occurrence of the studied phenomenon.

As highlighted by Sarricolea et al. (2020), preventive actions cannot be limited only to information campaigns and to the management of combustible material. Instead, they must include the planning of land use and occupation in terms of extension, aggregation, density and continuity, so as to prevent large-scale fires, especially in the most populated areas. Therefore, risk mapping, in addition to providing support for operational issues, must be taken into account by public administrators in their assessment of strategic issues, such as housing and project implementation.

This work aimed to map the fire propagation within the domains of the Itacolomi State Park, in Minas Gerais State, in a GIS environment, by comparing the variables of incident solar radiation with the aspect of the slopes, and also to analyze their efficiency for obtaining the best fire propagation risk map.

Material and methods

Study area

Created on June 14, 1967 by State Law n°. 4,495, the Itacolomi State Park (ISP) is located in the municipalities of Ouro Preto and Mariana, Minas Gerais State, Brazil (Figure 1). The park total area is 6,000.25 ha, 4,183.15 of which are within the limits of Mariana (IEF - Instituto Estadual de Florestas, 2007).

The Park is located in the southern portion of the *Reserva da Biosfera da Serra do Espinhaço*, in a transition region between the Cerrado and Atlantic Forest biomes, with two phytophysiological types, grasslands (high altitude and rupestrian fields) and forests, that are represented by the High Montane Semideciduous Forest and High Montane Ombrophylous Forest (Pedreira & De Sousa, 2011).

According to the Köppen climate classification, two types of climates are found in the ISP, Cwa and Cwb. Both have two well-defined seasons, rainy and dry (IEF, 2007).

Between 2013 and 2019, 57 fires were recorded within and around the ISP. The number of occurrences and the

extent of the burned area have increased, except for 2015 when no fire occurrence was recorded. The most critical

year was 2017, where both the number of occurrences and the number of burnt areas were highest in the period.

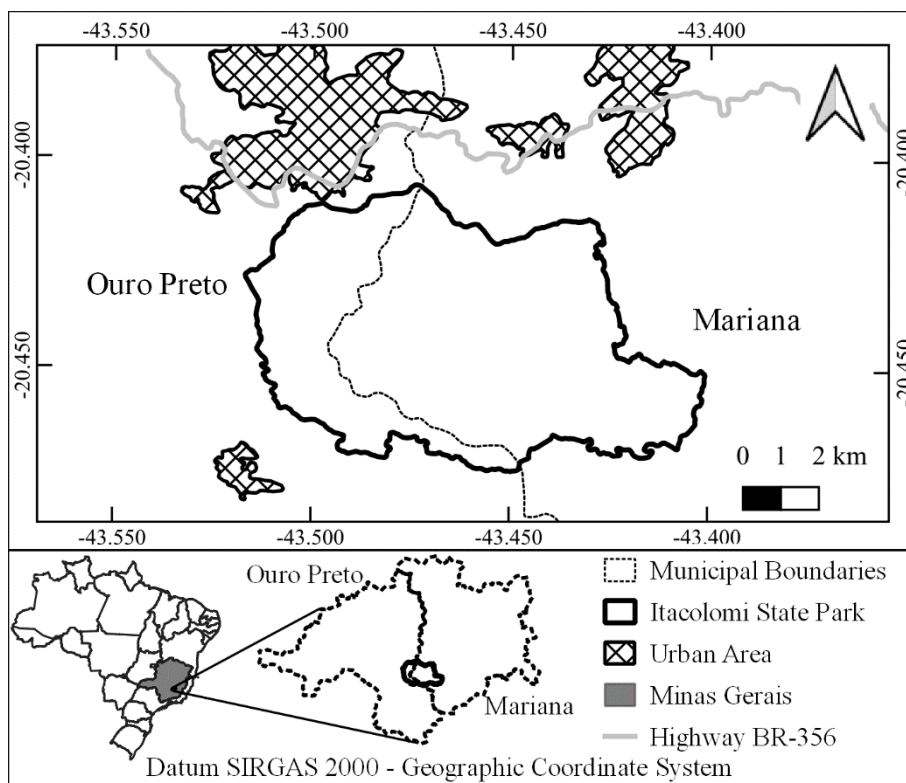


Figure 1. Study area map, highlighting, the Itacolomi State Park, Minas Gerais State, Brazil.

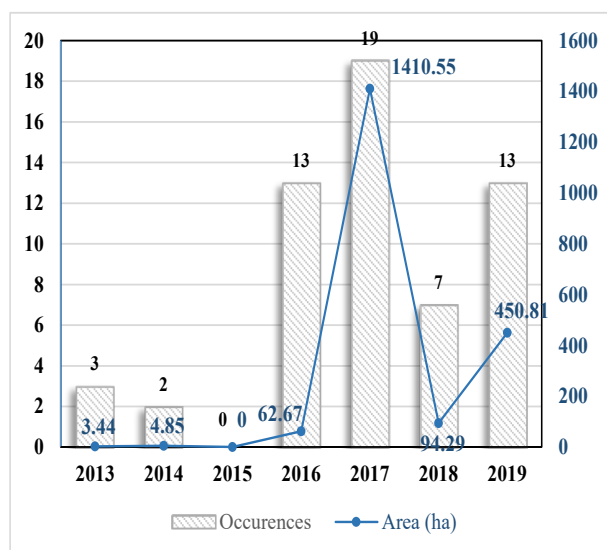


Figure 2. Evolution of fire occurrences and burnt area in the Itacolomi State Park, Minas Gerais State, Brazil, between 2013 and 2019.

Data set

The data on wildfires occurred within the limits of the ISP and its surroundings were provided by the Management of Prevention and Fire Fighting (Previncendio) of the *Instituto Estadual de Florestas of Minas Gerais* (IEF).

The fire occurrence record (ROI) is a document where the most diverse information related to a fire event is collected, enabling the systematization of this information and its statistical analysis, in order to define fire prevention and fighting strategies. This type of document was created in the 1990s by the *Centro Nacional de Prevenção e Combate aos Incêndios Florestais* (Prevfogo) of Ibama (*Instituto Brasileiro do Meio Ambiente e dos Recursos Naturais Renováveis*) and it has improved the quality of data collected in the field (Bontempo et al., 2011).

The ROI from 2012 to 2019 contain the following information: a) where the fire started; b) extension of the burned area; c) terrain data; d) detection and combat data; e) origin and cause; f) complementary observations; and g) source of the information. In addition to the ROI, vector files were available in the shapefile format of the burned areas between 2012 and 2019. However, no fires were detected inside the park in 2012 and 2015.

Description of the variables

There are several factors, physical and anthropogenic, that affect forest fires. As physics we can cite climatic factors, topography, drainage, soil texture, vegetation type and density. The anthropogenic are mainly the settlements and the connectivity of the area (Kayet et al., 2020).

Land cover/use (LCU) is an extremely important factor affecting fire ignition (Carmo et al., 2011). The presence or absence of plant material directly influences the risk of fire, as it serves as combustible material (Nicolete & Zimback, 2013). Vegetation types and density are important factors to analyze, as carbon content and other chemical components vary and can affect fire behavior (Kayet et al., 2020).

The image of the study area was obtained by the Sentinel-2 Level 2A satellite. The reference system used was SIRGAS 2000. The LCU map was obtained through supervised classification using the random forests model of the DZetsaka plugin and arranged in the following classes: water, rupestrian fields, eucalyptus, *candéal* (*Eremanthus erythropappus* area) and Semideciduous Forest (Figure 3).

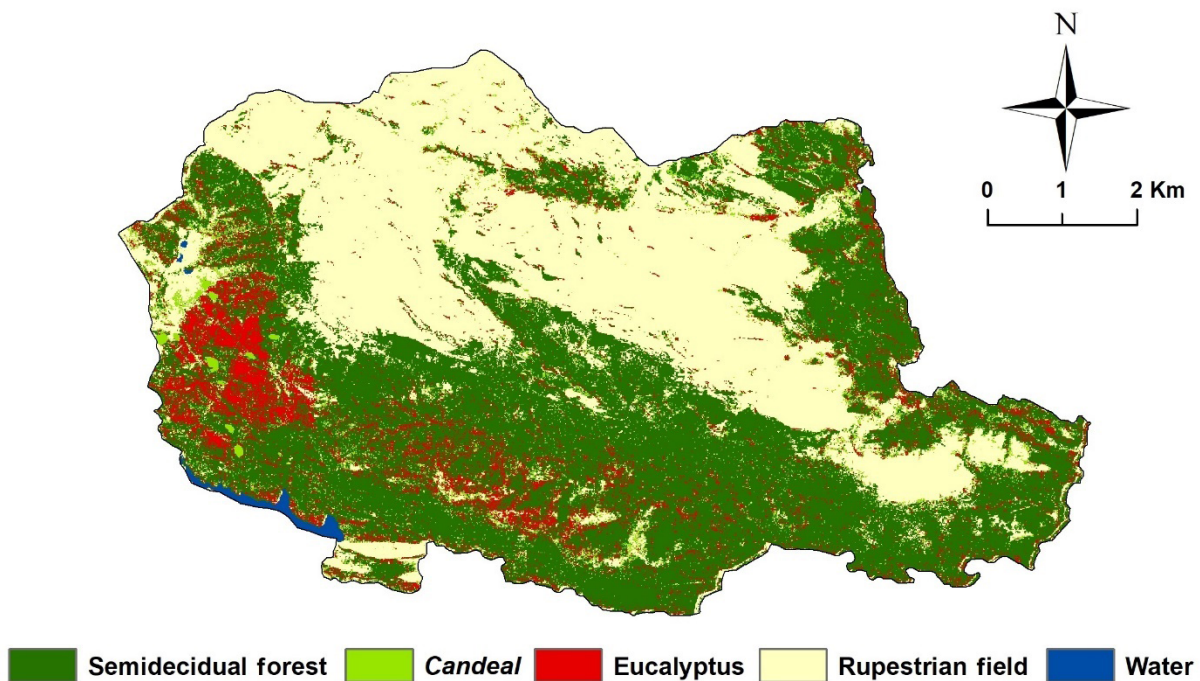


Figure 3. Land cover/use classification in Itacolomi State Park, Minas Gerais State, Brazil.

The contour lines of the study area were obtained from the Spatial Data Infrastructure of the State System for the Environment and Water Resources (IDE-Sisema), which uses the data from the project TOPODATA with a spatial resolution of 10 m and 30 m of equidistance. Afterwards, the digital elevation model (DEM) was generated from the contour lines through the *Create Tin* tool, on *ArcGIS 10.8* (Esri, 2012).

The study area altitude ranged from 600 m to 1,700 m. The DEM data were used to generate the variables related to the topography (slope, aspect, slope curvature and incident solar radiation). Areas with steeper slopes are considered more susceptible to fire propagation due to easier heat transfer towards the slope, which increases the speed of fire propagation (Leal et al., 2019). The slope variable was obtained in the *ArcGIS 10.8* (Esri, 2012) software system from the DEM file, and it was reclassified into five classes (Table 1), using the equal-interval reclass option of the Idrisi reclass function.

The aspect (ASP) is of great importance due to its relationship with solar radiation conditions, besides influencing the type and moisture of the fuel material (Eugenio et al., 2016; Çolak & Sunar, 2020). According to Soares et al. (2017), the southern hemisphere presents higher incidence of sunlight on the north face of the slopes, thus receiving and transmitting more energy

than the other exposures, which increases fire ignition risk. The orientation of the slopes (aspect) was obtained from the MDE, using the *Aspect* tool on the *ArcGIS 10.8* (Esri, 2012) software system (Table 1).

According to Andrade & Ferreira (2019), solar radiation is able to reveal characteristics of humidity and dryness of the vegetation cover. The calculation of incident solar radiation (SOL) is related to the local latitude. To determine this variable, the period from June 1 to September 30, which covers the driest months of the year, was analyzed. The total radiation was obtained by the *Area Solar Radiation* tool in the *ArcGIS 10.8* (Esri, 2012) software system.

Through variations in the geomorphological characteristic, it is possible to highlight areas within slopes somewhat propitious to the occurrence of fires, which are encompassed in three main forms: concave, convex and rectilinear. The concave shapes are those with the highest concentration of moisture, due to the flow convergence zones, while the convex and rectilinear forms present low humidity because they condition the formation of divergence zones (Andrade & Ferreira, 2019). The slope curvature (CUR) was obtained from TOPODATA (Inpe, 2011), cropped to the study area and classified into 5 classes on *ArcGIS 10.8* software system.

Table 1. Explanatory variables used in the fire propagation risk mapping of the Itacolomi State Park, Minas Gerais State, Brazil.

Variables				
Aspect (°)	Slope (°)	Radiation (WH m ⁻²)	Slope curvature	Land cover/use
Flat (-1)	0-15	23 - 45.2	Very concave	Water
North (0-22.5; 337.5 – 360)	15-30	45.2 - 67.4	Concave	Eucalyptus
Northeast (22.5-67.5)	30-45	67.4 - 89.6	Rectilinear	<i>Candea</i>
East (67.5-112.5)	45-60	89.6 - 111.8	Convex	Rupestrian field
Southeast (112.5-157.5)	> 60	111.8 - 134.0	Very convex	Semideciduous Forest
South (157.5-202.5)				
Southwest (202.5-247.5) (202.5-247.5)				
West (247.5-292.5)				
Northwest (292.5-337.5)				

Fire propagation risk mapping

The fire propagation risk mapping was performed using the multicriteria analysis method on GIS. After the processing of the variables, which was carried out using the softwares *ArcGIS 10.8* (Esri, 2012) and *Idrisi Selva 17.0* (Eastman, 2012), the weight for each class was assigned and its respective total and burned area

were calculated, defining the percentage of burned area in the class. Subsequently, the class with the largest burned area was defined by the authors as weight 10, while the others were calculated proportionally (Table 2). For representative purposes, the second class (C_{i+1}) was defined as the class with the highest burning percentage.

Table 2. Explanatory table for the assignment of weights of each class to the explanatory variables.

Variable	Class	Area (ha)	Burned area (ha)	Burned area (%)	Weight
V_i	C_i	Area C_i	Burned area C_i	$\frac{\text{Burned area } C_i \times 100}{\text{Total area } C_i}$	$\frac{\% \text{Burned area } C_i \times 10}{\% \text{Burned area } C_{i+1}}$
	C_{i+1}	Area C_{i+1}	Burned area C_{i+1}	$\frac{\text{Burned area } C_{i+1} \times 100}{\text{Total area } C_{i+1}}$	10*
	C_{i+2}	Area C_{i+2}	Burned area C_{i+3}	$\frac{\text{Burned area } C_{i+2} \times 100}{\text{Total area } C_{i+2}}$	$\frac{\% \text{Burned area } C_{i+2} \times 10}{\% \text{Burned area } C_{i+1}}$

V_i =: Variables i ; C_i = Variable class i ; *Weight 10 was attributed to the variable with highest % burned area.

After weight calculation, the LCU, STR and ASP maps were overlapped, within the image calculator function, from *Idrisi*, generating the first ignition risk map, and the LCU, STR and SOL maps, as the second fire ignition risk map. The proportion of the LCU variable for the other variables was defined as 3:1, since the fuel type has the strongest effect on fire ignition. Afterwise, the ignition maps were crossed with the slope (SLP) in a 1:1 proportion, generating two final maps, which were reclassified into five propagation risk classes, using the equal-interval reclass option of the *Idrisi* reclass function.

Validation

The validation was performed from real fire data from 2016 to 2019, in order to verify the efficiency of the fire propagation risk maps. The final maps were reclassified into two classes (susceptible and non-susceptible),

according to Table 3. Likewise, the real fire map was also classified into two classes (burned and unburned areas) for validation purposes. In addition, the moderate class had two distinct approaches, estimating two areas under the curve (AUC), considering it as susceptible and non-susceptible.

Table 3. Fire propagation risk classes for the modeled and real fire maps.

Fire propagation risk	Classification
Very high	Susceptible
High	Susceptible
Moderate (considered in two different ways for validation)	Susceptible / non-susceptible
Low	Non-susceptible
Very low	Non-susceptible

Based on the classification performed for the two fire propagation risk maps, the AUC method (Equation 1) was used for the susceptible classes, considering the moderate class as susceptible and non-susceptible, to be compared afterwise. The AUC method summarizes the interpretation of a receiver operating characteristic (ROC) curve (Bradley, 1997). The AUC can be interpreted as the probability that a burned area randomly chosen will be classified as susceptible in relation to an unburned area. Values below 0.6 mean that the model is not suitable; values between 0.6 and 0.7 indicate poor performance; between 0.7 and 0.8, moderate performance; between 0.8 and 0.9, good performance; and between 0.9 and 1.0, it means that the performance of the model is excellent (Ngoc Thach et al., 2018; Tien Bui et al., 2018).

$$AUC = \frac{\frac{TP}{(TP - FN)} - \frac{FP}{(FP + TN)} + 1}{2} \quad (1)$$

Where: AUC = area under the curve; TP = burned areas classified as susceptible (true positive); FN = burned area classified as non-susceptible (false negative); FP = areas classified as susceptible that did not burn (false positive); TN = areas that did not burn and were classified as “non susceptible” (true negative).

Finally, the AUC values and the behavior of the classes were compared to determine the best variable (ASP or SOL) for mapping fire propagation risk.

Results

Analysis of variables and their weights.

The weights obtained for each class of variables are presented in Table 4.

The analysis of the aspect (ASP) reveals that the slopes facing North (NW, N and NE) presented the largest burned extension, although the West face has the second largest burned area, proportionally, which allowed it to obtain the second highest weight. When analyzing the slope (SLP), the class 0-15 presented a greater burned area, both in extension and in proportion. Also, the results of the incident solar radiation (SOL)

are consistent with the expected where the areas exposed to greater solar radiation were more burned, both in extension and proportion. The results also revealed that the very convex class presented the largest burned area, in length and proportion. The convex class had the second largest burned area in extension, but received the lowest score in the variable, since the very concave and concave classes obtained, proportionally to their total areas, a greater burned area percentage. In relation to land cover/use, the rupestrian field class was the most affected by the occurrence of fire, presenting 34.7% of its area burned.

Fire propagation maps

The fire ignition risk maps using ASP and SOL were generated separately and crossed with the SLP map with the Image calculator, and further reclassified into five classes. Figure 4 illustrates the fire ignition, slope and fire propagation maps.

The analysis of both ignition risk maps reveals that the areas with predominant rupestrian fields presented the highest risk (Figures 3 and 4). It is important to note that, when comparing the slope map with both propagation risk maps, the least fire prone areas are those with the lowest slope class (0-15). Also, when comparing the ignition maps, it reveals that both are similar in most of the territory. The difference between the two maps is mainly observed in the moderate and high classes. In the ASP ignition fire map, there is a larger area of the high class in relation to the SOL map, which in turn has a larger area of the moderate class. These differences become almost imperceptible when the final propagation maps are compared.

Validation

The area under the curve values found for the fire propagation risk maps were very similar for both methods (ASP and SOL) in both approaches (moderate class as susceptible and not susceptible to fires). When considering the moderate class as susceptible, the AUC values were 0.758 for Aspect and 0.763 for the Solar Radiation methods. On the other hand, when considering the moderate class as not susceptible, the AUC values obtained were 0.583 and 0.578 for Aspect and Solar Radiation methods, respectively.

Table 4. Weight calculated for each class of the variables used in the fire propagation risk mapping of the Itacolomi State Park, Minas Gerais State, Brazil.

Variable	Class	Area (ha)			Burned area (%)	Weight
		Total	Burned (1x)	Burned (2x)		
ASP	Flat	604.54	94.69	0.00	15.7	4.3
	North	560.83	141.83	2.51	26.2	7.1
	Northeast	902.29	187.34	0.52	20.9	5.7
	East	787.23	124.92	0.06	15.9	4.3
	Southeast	876.87	93.92	0.00	10.7	2.9
	South	1056.87	67.46	0.00	6.4	1.7
	Southwest	546.70	48.05	0.01	8.8	2.4
	West	275.79	74.01	0.83	27.4	7.5
	Northwest	347.63	123.16	2.21	36.7	10
SLP	0-15	2.304.59	502.65	2.4	22.0	10
	15-30	2.925.55	378.15	1.95	13.1	5.9
	30-45	695.69	69.53	1.28	10.4	4.7
	45-60	32.43	5.02	0.51	18.6	8.5
	> 60	0.49	0.03	0.00	6.1	2.8
SOL	23 - 45.2	16.87	0.05	0.00	0.3	0.1
	45.2 - 67.4	269.59	8.12	0.00	3.0	1.1
	67.4 - 89.6	1.256.97	83.93	0.15	6.7	2.4
	89.6 - 111.8	2.564.18	344.35	1.19	13.5	4.8
	111.8 - 1340	1.888.08	524.56	5.00	28.3	10
CUR	Very concave	416.36	71.36	0.15	17.2	8.8
	Concave	258.93	46.46	0.20	18.1	9.2
	Rectilinear	423.01	67.05	0.13	15.9	8.1
	Convex	2.716.14	358.69	1.08	13.3	6.8
	Very convex	2.158.26	414.67	4.74	19.7	10
LCU	Water	27.61	0.00	0.00	0.0	0.0
	Eucalyptus	538.87	16.80	0.04	3.1	0.9
	<i>Candea</i>	312.42	25.82	0.00	8.3	2.4
	Rupestrian field	2.380.25	814.36	6.18	34.7	10
	Semideciduous Forest	2.736.20	102.09	0.02	3.7	1.1

ASP= aspect; SLP= slope; SOL= incident solar radiation; CUR= slope curvature; LCU= land cover/use; *Weight 10 attributed to the highest % burned area.

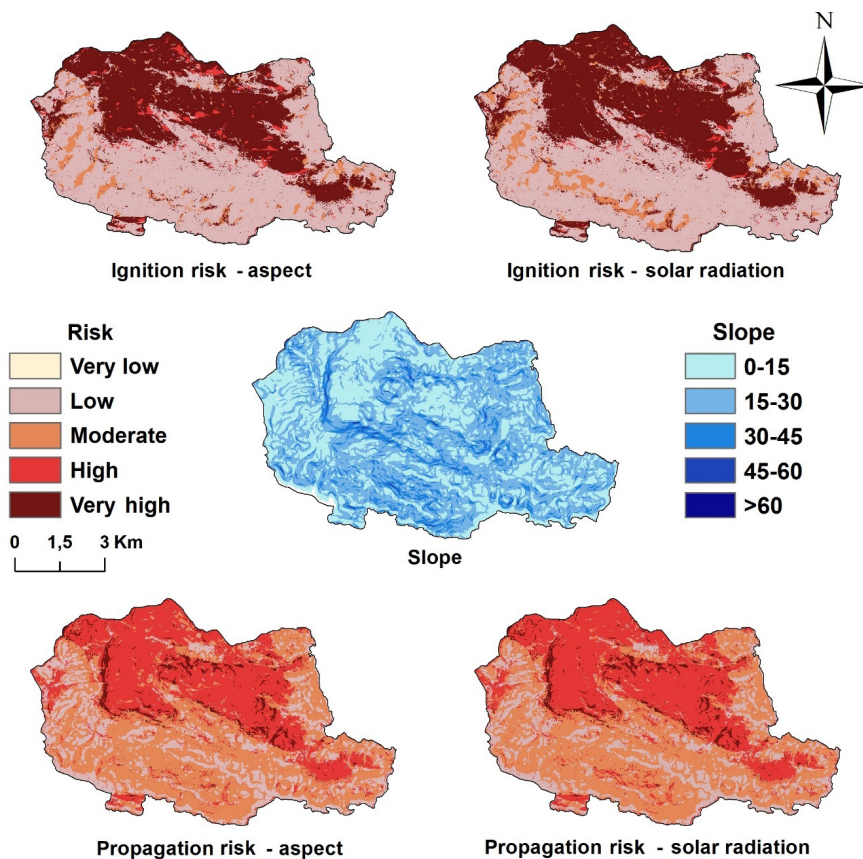


Figure 4. Ignition, slope and fire propagation maps with the aspect and solar radiation variables in Itacolomi State Park, Minas Gerais State, Brazil.

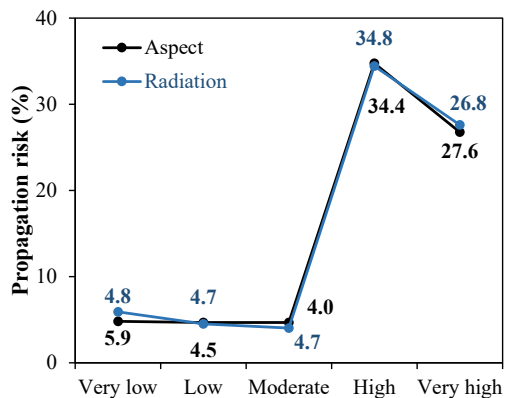


Figure 5. Relative area burned from 2014 to 2019 by fire propagation risk class defined by the aspect and solar radiation methods in Itacolomi State Park, Minas Gerais State, Brazil.

Discussion

In this study, we evaluated two fire propagation risk mapping methods using fire frequency data from the Itacolomi State Park (ISP), located in Minas Gerais State, Brazil, and four variables for each method. The variables presented different behaviors when applying them to model fire propagation risk.

The slope orientation is related to the solar radiation variable, which is also related to heat stroke and, thus, indirectly to temperature and humidity, which implies on higher susceptibility with higher ray incidence. It should be noted that dead fuel material is more susceptible to climatic factors (Torres et al., 2017). Therefore, the exposure of these materials to more intense and prolonged radiation will make them more fire prone

(Bacani, 2016). The maps presented a higher burned area on the slopes facing north, which is expected, since in the southern hemisphere the sun's rays fall with greater intensity on the faces facing north, transmitting more heat to them, compared to the others (Fernandes Filho & Sá, 2007). Despite this information, there may be exceptions, such as Ladislau et al. (2021) study, also carried out in Minas Gerais State, which the south, southeast and southwest slope orientations were more fire prone. The west face is the second in the amount of heat received, followed by the east face, while the south face receives the least amount of radiation (Torres et al., 2014), in opposition to what is observed in the northern hemisphere, where the slopes facing south are more prone to burning, as demonstrated by Sari (2020).

The slope variable is mainly related to fire spread and greatly affects the behavior of the fire (Soares Neto et al., 2016). It facilitates the preheating of the fuel in the slope areas as a result of a greater proximity of the flames to the vegetation. Thus, the greater the slope in the direction of the fire line propagation, the higher is the spread rate (Carmo et al., 2011; Marchesan et al., 2020). However, the work presented an opposite behavior, since the lowest slopes were more fire-prone, leading to the conclusion that, in the studied area, other variables seem to be more influential on the occurrence of fire than the slope. The same result was obtained by Leal et al. (2019) in their study area, where the behavior of the slope with the highest risk classes accounted for 2.8% of the total area.

When evaluating the curvature variable, the very convex areas presented the largest burned area, followed by the convex slopes, which is expected, since the concave shapes present the highest concentration of moisture, due to the flow convergence zones, while the convex and rectilinear forms have low humidity because they condition the formation of divergence zones (Andrade & Ferreira, 2019).

The rupestrian field had the most burned area, because, in addition to the greater propensity of this physiognomy to fire (Le Stradic et al., 2015), the class is located in the north of the park, where there is a great anthropic pressure due to the expansion of urbanization, both in the municipality of Ouro Preto and Mariana. Therefore, the combination of greater propensity and proximity to urban settlements is the main cause of almost all fire events in the park. According to Duarte & Teodoro (2016) wildfires are strongly influenced not only by

environmental factors, but also by anthropic factors. Torres et al. (2017) pointed out that the population interferes in the annual cycles of fire, thereby reducing or increasing the season and areas most conducive to the occurrence of fires. According to Sarricolea et al. (2020), the growth of urban areas has increased the risk of fire, since it increases the areas called wildland-urban interface (WUI).

In both maps, there is a great continuity in the high class, which extends from the north boundary towards the southeast region of the ISP (Figure 4). This continuity of the class is due to the rupestrian fields. Since the continuity of the combustible material is one of the main factors linked to the spread of wildfires (Novo et al., 2020), it is clear that this region needs greater attention from administrators in order to prevent the occurrence of uncontrolled fires.

The dimensioning of WUI can support territorial planning focused on mitigation and adaptation, so as to enable the creation of surveillance systems, forest fire prevention protocols, housing protection systems and the use of prescribed fire (Sarricolea et al., 2020). The same authors indicated that the design of WUI involves the mapping of combustible material and the population potentially affected. Therefore, it is understood that the determination of the WUI close to the ISP would have a synergistic effect with the fire propagation risk map, also allowing decision makers to choose and / or to develop the best strategies aimed at preserving the ISP and the surrounding community.

When evaluating the precision of the maps, the area under the curve (AUC) method was applied. Many studies mention the use of this validation method (Pourtaghi et al., 2016; Gholamnia et al., 2020; Rodrigues et al., 2020; Santana Neto et al., 2022). Pourtaghi et al. (2016), for example, used the AUC method to evaluate three different modeling methods, boosted regression tree (BRT), generalized additive model (GAM) and random forest (RF), which were used to discriminate between absence or presence of wildfires, with performances peaking at AUC of 0.8084, 0.8770 and 0.7279, respectively. When the moderate class was considered not susceptible to fires, the maps showed moderate precision, whereas when the same class was considered non-susceptible, the precision of the model was considered adequate (Ngoc Thach et al., 2018; Tien Bui et al., 2018), which makes it suitable to explain the occurrence of fires, although the risk may be underestimated.

As observed in Figure 5, the relative areas burned largely coincided with the fire risk classes of most concern (high and very high) in both methods, which demonstrates that the predictor variables were able to satisfactorily map the areas with the highest fire propagation risk. Chang et al. (2013) obtained a similar result in modeling the occurrence of fires in Heilongjiang province (China) and achieved an overall accuracy of 64,9%.

This research used a dataset obtained from official databases, which makes it easily replicable for other areas of study. However, the low availability of historical fire data can be considered a limitation to the study. For this reason, future studies should use long-term data of fires occurrence, and it is also strongly recommended that future studies consider the differences between the incidence of solar radiation and the orientation of the slopes, since, although the results in the present study area are similar, they may differ for other locations.

Conclusions

This work evaluated the efficiency of fire propagation risk methods in two different approaches, where the moderate class was defined as susceptible in one approach, and non-susceptible in the other. The fire propagation risk maps obtained when the moderate class was considered susceptible did not present adequate precision for any of the methods (aspect and incidence of solar radiation). On the other hand, when the moderate class was considered non-susceptible, the results showed moderate accuracy. In addition, both methods showed very similar area under the curve values for the two variables used.

Finally, the burned area increased according to the fire propagation risk in both methods presenting the high and very high classes with the highest percentages of fire propagation risk. Therefore, the results obtained in this study can be used to assist in adopting fire mitigation measures in the most susceptible areas, mainly rupestrian field areas.

Acknowledgements

This study was financed in part by the Coordenação de Aperfeiçoamento de Pessoal de Nível Superior - Brasil (CAPES) - Finance Code 001.

Conflict of interest

The authors have no conflict of interest to declare.

Authors' Contributions

Vicente Paulo Santana Neto: Conceptualization, formal analysis, investigation, methodology, supervision, writing – original draft, writing – review & editing.

David Marques Soares: Formal analysis, investigation, methodology, writing – original draft, writing – review & editing.

Thais Camargos da Silva: Formal analysis, writing – original draft, writing – review & editing.

Fillipe Tamiozzo Pereira Torres: Writing – review & editing.

References

- Andrade, S. C. & Ferreira, A. F. Mapeamento geoecológico da susceptibilidade à ocorrência de incêndios no Parque Estadual da Serra da Concórdia – Valença RJ. **Revista Eletrônica TECCEN**, v. 12, n. 2, p. 45-58, 2019. <http://dx.doi.org/10.21727/teccen.v12i2.1999>.
- Bacani, V. M. Geoprocessing applied to risk assessment of forest fires in the municipality of Bodoquena, Mato Grosso do Sul. **Revista Árvore**, v. 40, n. 6, p. 1003-1011, 2016. <http://dx.doi.org/10.1590/0100-67622016000600005>.
- Bontempo, G. C. et al. Registro de Ocorrência de Incêndio (ROI): evolução, desafios e recomendações. **Biodiversidade Brasileira**, v. 1, n. 2, p. 247-263, 2011.
- Bradley, A. P. The use of the area under the ROC curve in the evaluation of machine learning algorithms. **Pattern Recognition**, v. 30, n. 7, p. 1145-1159, 1997. [http://dx.doi.org/10.1016/S0031-3203\(96\)00142-2](http://dx.doi.org/10.1016/S0031-3203(96)00142-2).
- Carmo, M. et al. Land use and topography influences on wildfire occurrence in northern Portugal. **Landscape and Urban Planning**, v. 100, n. 1-2, p. 169-176, 2011. <http://dx.doi.org/10.1016/j.landurbplan.2010.11.017>.
- Chang, Y. et al. Predicting fire occurrence patterns with logistic regression in Heilongjiang Province, China. **Landscape Ecology**, v. 28, n. 10, p. 1989-2004, 2013. <http://dx.doi.org/10.1007/s10980-013-9935-4>.
- Çolak, E. & Sunar, F. Evaluation of forest fire risk in the Mediterranean Turkish forests: a case study of Menderes region, Izmir. **International Journal of Disaster Risk Reduction**, v. 45, p. 101479, 2020. <http://dx.doi.org/10.1016/j.ijdr.2020.101479>.
- Duarte, L. & Teodoro, A. C. An easy, accurate and efficient procedure to create forest fire risk maps using the SEXTANTE plugin Modeler. **Journal of Forestry Research**, v. 27, n. 6, p. 1361-1372, 2016. <http://dx.doi.org/10.1007/s11676-016-0267-5>.
- Eastman, J. R. **IDRISI Selva Manual**. 17.01 ed. Clark University, 2012. 324 p.

- Edwards, A. C. et al. A comparison and validation of satellite-derived fire severity mapping techniques in fire prone north Australian savannas: extreme fires and tree stem mortality. **Remote Sensing of Environment**, v. 206, p. 287-299, 2018. <http://dx.doi.org/10.1016/j.rse.2017.12.038>.
- ESRI. **ArcGIS Desktop**: Release 10.8. Redlands, CA: Instituto de Pesquisa de Sistemas Ambientais, 2011.
- Eugenio, F. C. et al. Applying GIS to develop a model for forest fire risk: a case study in Espírito Santo, Brazil. **Journal of Environmental Management**, v. 173, p. 65-71, 2016. <http://dx.doi.org/10.1016/j.jenvman.2016.02.021>.
- Fernandes Filho, E. I. ; & Sá, M. M. F. Influência das variáveis do terreno na radiação solar. In: Simpósio Brasileiro de Sensoriamento Remoto, 13., 2007. **Anais [...]**. Florianópolis: INPE, 2007. p. 5751-5753.
- Gholamnia, K. et al. Comparisons of diverse machine learning approaches for wildfire susceptibility mapping. **Symmetry**, v. 12, n. 4, p. 1-20, 2020. <http://dx.doi.org/10.3390/SYM12040604>.
- Guglietta, D. et al. A Multivariate approach for mapping fire ignition risk: the example of the National Park of Cilento (Southern Italy). **Environmental Management**, v. 56, n. 1, p. 157-164, 2015. <http://dx.doi.org/10.1007/s00267-015-0494-0>.
- ICMBio. Instituto Chico Mendes de Conservação da Biodiversidade. **Incêndios em Unidades de Conservação Federais**. Disponível em: <https://dados.gov.br/dataset/incendios-em-ucs>. Acesso em: 9 fev. 2021.
- IEF. Instituto Estadual de Florestas. **Plano de manejo**: Parque Estadual do Itacolomi. Belo Horizonte: Secretaria de Meio Ambiente de Minas Gerais, 2007. Disponível em: <http://www.ief.mg.gov.br/component/content/193?task=view>. Acesso em: 03 mar. 2022.
- INPE. Instituto Nacional de Pesquisas Espaciais. **TOPODATA**: Banco de Dados Geomorfométricos do Brasil. Disponível em: <http://www.dsr.inpe.br/topodata/index.php>. Acesso em: 8 nov. 2021.
- Kayet, N. et al. Comparative analysis of multi-criteria probabilistic FR and AHP models for forest fire risk (FFR) mapping in Melghat Tiger Reserve (MTR) forest. **Journal of Forestry Research**, v. 31, n. 2, p. 565-579, 2020. <http://dx.doi.org/10.1007/s11676-018-0826-z>.
- Ladislau, F. F. et al. Análise multicritério aplicada ao mapeamento de risco de incêndio na APA Sul RMBH. **Caderno de Geografia**, v. 31, n. 66, p. 667, 2021. <http://dx.doi.org/10.5752/p.2318-2962.2021v31n66p667>.
- Leal, F. A. et al. Zoneamento de riscos de incêndios florestais em regiões hot spot de focos de calor no estado do Acre. **Nativa**, v. 7, n. 3, p. 274, 2019. <http://dx.doi.org/10.31413/nativa.v7i3.6768>.
- Le Stradic, S. et al. Diversity of germination strategies and seed dormancy in herbaceous species of campo rupestre grasslands. **Austral Ecology**, v. 40, n. 5, p. 537-546, 2015. <http://dx.doi.org/10.1111/aec.12221>.
- Leuenberger, M. et al. Wildfire susceptibility mapping: deterministic vs. stochastic approaches. **Environmental Modelling and Software**, v. 101, p. 194-203, 2018. <http://dx.doi.org/10.1016/j.envsoft.2017.12.019>.
- Marchesan, J. et al. Risco de incêndios na Estação Ecológica do Taim, Rio Grande do Sul. **Nativa**, v. 8, n. 1, p. 112, 2020. <http://dx.doi.org/10.31413/nativa.v8i1.8180>.
- Ngoc Thach, N. et al. Spatial pattern assessment of tropical forest fire danger at Thuan Chau area (Vietnam) using GIS-based advanced machine learning algorithms: a comparative study. **Ecological Informatics**, v. 46, p. 74-85, 2018. <http://dx.doi.org/10.1016/j.ecoinf.2018.05.009>.
- Nicolete, D. A. P. & Zimback, C. R. L. Zoneamento de risco de incêndios florestais para a fazenda experimental Edgardia – Botucatu (SP), através de sistemas de informações geográficas. **Revista Agrogeoambiental**, v. 5, n. 3, p. 55-62, 2013. <http://dx.doi.org/10.18406/2316-1817v5n32013518>.
- Novo, A. et al. Automatic processing of aerial LiDAR data to detect vegetation continuity in the surroundings of roads. **Remote Sensing**, v. 12, n. 10, p. 1-14, 2020. <http://dx.doi.org/10.3390/rs12101677>.
- Pedreira, G. & De Sousa, H. C. Comunidade arbórea de uma mancha florestal permanentemente alagada e de sua vegetação adjacente em Ouro Preto-MG, Brasil. **Ciencia Florestal**, v. 21, n. 4, p. 663-675, 2011. <http://dx.doi.org/10.5902/198050984511>.
- Pourtaghi, Z. S. et al. Investigation of general indicators influencing on forest fire and its susceptibility modeling using different data mining techniques. **Ecological Indicators**, v. 64, p. 72-84, 2016. <http://dx.doi.org/10.1016/j.ecolind.2015.12.030>.
- Rodrigues, M. et al. Geospatial modeling of containment probability for escaped wildfires in a Mediterranean Region. **Risk Analysis**, 2020. <http://dx.doi.org/10.1111/risa.13524>.
- Santana Neto, V. P. et al. Burning susceptibility modeling to reduce wildfire impacts: a GIS and multivariate statistics approach. **Floresta e Ambiente**, v. 29, n. 1, p. 1-12, 2022. <http://dx.doi.org/10.1590/2179-8087-FLORAM-2021-0078>.
- Sari, F. Forest fire susceptibility mapping via multi-criteria decision analysis techniques for Mugla, Turkey: a comparative analysis of VIKOR and TOPSIS. **Forest Ecology and Management**, v. 480, p. 118644, 2020. <http://dx.doi.org/10.1016/j.foreco.2020.118644>.
- Sarricolea, P. et al. Recent wildfires in Central Chile: detecting links between burned areas and population exposure in the wildland urban interface. **Science of the Total Environment**, v. 706, p. 135894, 2020. <http://dx.doi.org/10.1016/j.scitotenv.2019.135894>.
- Soares Neto, G. B. et al. Riscos de incêndios florestais no parque nacional de Brasília, Brasil. **Territorium**, n. 23, p. 161-170, 2016. http://dx.doi.org/10.14195/1647-7723_23_13.
- Soares, R. V. et al. **Controle, efeitos e uso do fogo**. 2. ed. Viçosa, MG: Produção Independente, 2017.
- Tien Bui, D. et al. GIS-based spatial prediction of tropical forest fire danger using a new hybrid machine learning method. **Ecological Informatics**, v. 48, p. 104-116, 2018. <http://dx.doi.org/10.1016/j.ecoinf.2018.08.008>.
- Torres, F. T. P. et al. Mapeamento da suscetibilidade a ocorrências de incêndios em vegetação na área urbana de Ubá-MG. **Revista Árvore**, v. 38, n. 5, p. 811-817, 2014. <http://dx.doi.org/10.1590/S0100-67622014000500005>.
- Torres, F. T. P. et al. Mapeamento do risco de incêndios florestais utilizando técnicas de geoprocessamento. **Floresta e Ambiente**, v. 24, 2017. <http://dx.doi.org/10.1590/2179-8087.025615>.